



Summer Student Program
at Joint Institute for Nuclear Research

Veksler and Baldin Laboratory of High Energy Physics

**Beam transport line from the Heavy Ion
Linear Accelerator to the Nuclotron ring for
the NICA project.**

Bulanov Andrey
Orlov Artem
Pomogaybo Grigory
NRNU MEPHI

Supervisors: PhD Butenko Andrey Valerievich

PhD Sidorin Anatoly Olegovich

Researcher Tuzikov Alexei Vasilevich

Dubna, 2015

Content

Introduction.....	3
Nuclotron based Ion Collider (NICA project)	3
Heavy Ion Linac (HILac).....	6
Geometry of the transport channel.....	9
Angle optimisation.....	10
Transport channel design in MAD-X	11
Beam dynamics.....	13
Conclusions.....	15
Acknowledgement.....	16
References	16

Introduction

The construction of the linear accelerator for heavy ions NICA Project will be finished in September 2015. Since the construction of the booster ring will be completed only in 2018 it was proposed to use a linear accelerator as an injector for the Nuclotron. In order, to inject heavy ions in the existing circular accelerator it is necessary to build a transport channel.

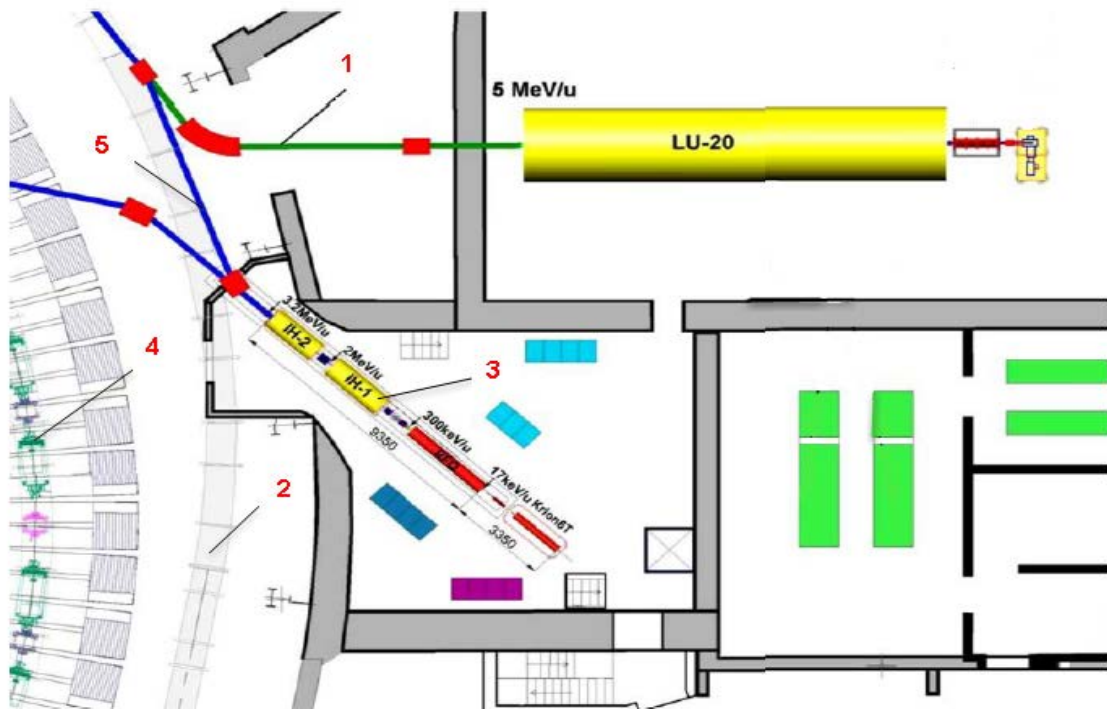


Figure 1.1 Injection facility: 1 – LU-20 injection; 2 – NUCLOTRON; 3 – HILAC; 4 – Booster ring; 5 – Transport channel.

Nuclotron based Ion Collider (NICA project)

Project NICA/MPD (Nuclotron based Ion Collider facility and Multi Purpose Detector) is an accelerator facility conceived to implement a world-leading program in particle physics at JINR. A description of the physics program envisioned is available on the web.

Project NICA/MPD is a part of the JINR Roadmap for 2009-2016 is described in the JINR 7-years Program. It is approved by Scientific Council of JINR and The Committee of Plenipotentiaries of JINR in 2009. That is a flagship project of JINR presently.

The project comprises experimental studies of fundamental character in the fields of the following directions of experimental research[1]:

1. Relativistic nuclear physics — search for mixed phase, phase transitions and critical phenomena in strongly interacting baryonic matter;
2. Spin physics in high and middle energy range of interacting particles;
3. Radiobiology.

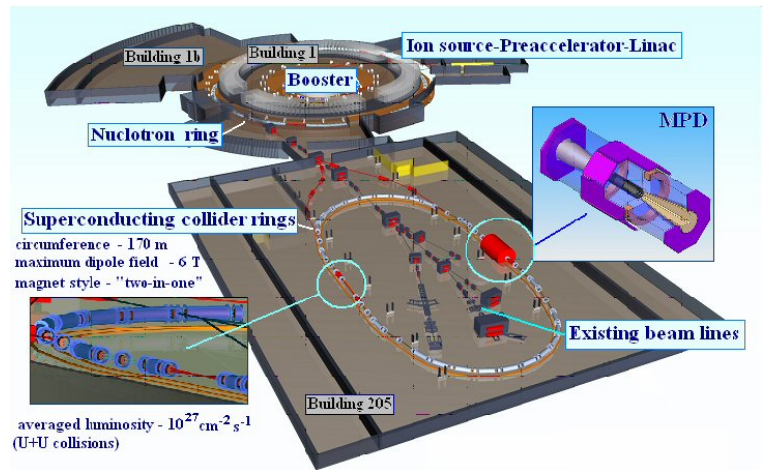


Figure 2.1 NICA-project

NICA complex includes the following main elements:

- injection complex;

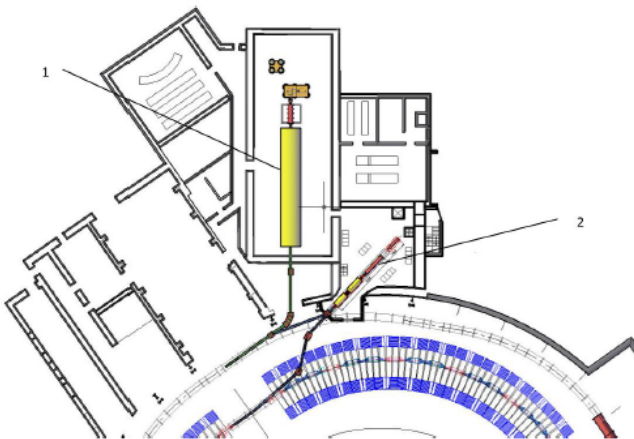


Figure 2.2 Structure of the injection complex: 1 - Linear accelerator LU-20; 2 - heavy ion accelerator HILAC.

It created for:

- injection into the Booster beams of heavy ions with a charge to mass ratio $q / A = 1/6$ and energy 3.2 MeV / n;
- injection into the Nuclotron beams of light ions with charge to mass ratio $q / A = 1/3$ and polarized deuterons and protons with energies of 5 MeV / n.[1]

- superconducting synchrotron - booster;

Main objectives:

Accumulation of 2×10^9 gold $^{197}\text{Au}^{31+}$ ions and accelerating them to an energy 578 MeV / n, which is sufficient for the subsequent stripping them to the state $^{197}\text{Au}^{79+}$. [2]

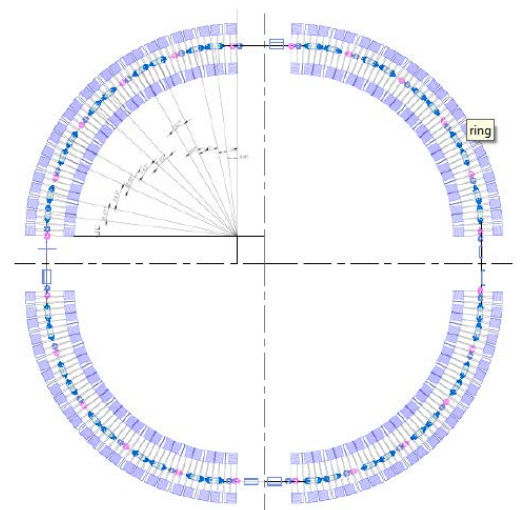


Figure 2.3 Booster ring in Synchrophasotron tunnel

- existing superconducting synchrotron Nuclotron;

Nuclotron superconducting proton synchrotron with maximum magnetic rigidity 45 T·m, accelerating heavy ions up to energy $1 \div 4,5 \text{ GeV} / n$. The project NICA in recent years implemented program for the modernization of the main systems - the Nuclotron-M. Currently, Nuclotron provides now conducting experiments on beams of accelerated protons and nuclei (up to iron nuclei ($A = 56$) with energies up to $5.7 \text{ GeV} / n$ and $2.2 \text{ GeV} / n$ respectively.[2]

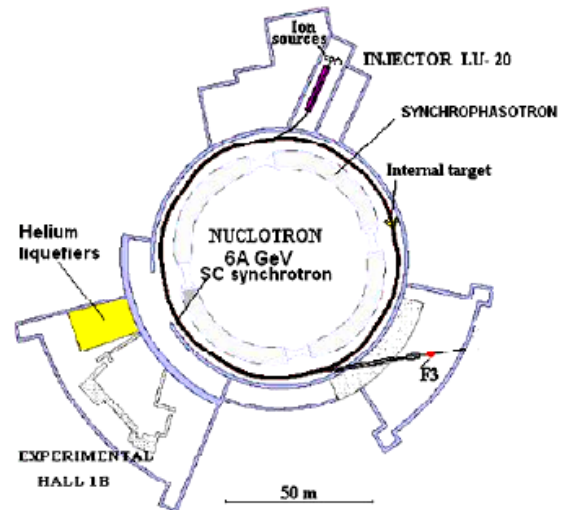


Figure 2.4 Nuclotron

- The collider, which consists of two superconducting ring with two points where beams faced;

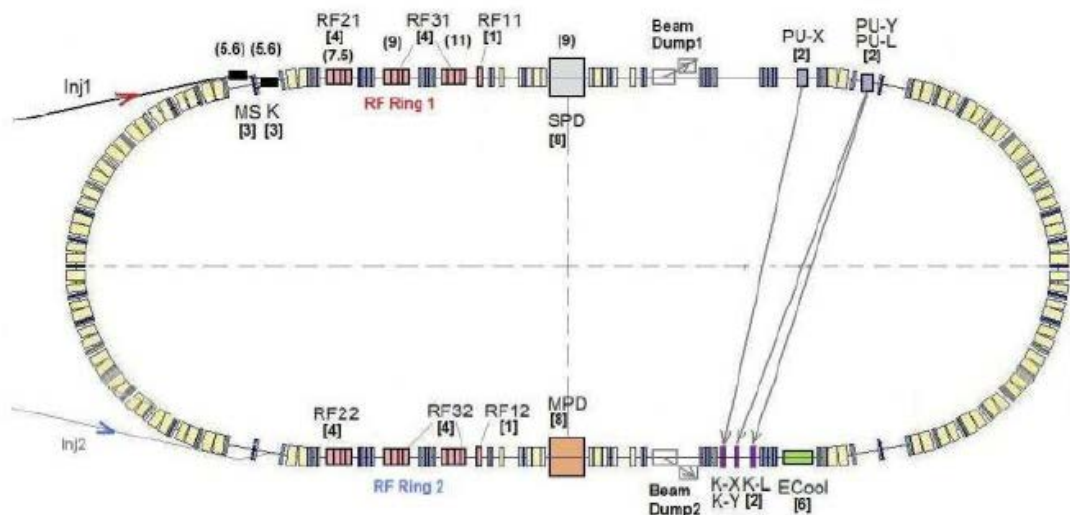


Figure 2.5 Collider scheme and the arrangement of equipment in the ring: RF - Station accelerating RF voltage, Beam Dump - beam system reset, PU - pick-up electrodes, K - correctors stochastic cooling system, ECool - electronic system cooling, MPD, SPD - Detectors

Collider designed for experiments on ion-ion and ion-proton collisions in the range of kinetic energies up to $1 \div 4,5 \text{ GeV} / n$, as well as polarized proton collisions ($5 \div 12,6 \text{ GeV} / n$) and deuterons ($2 \div 5.8 \text{ GeV} / n$). The main mode of the collider is collisions particles up to Au at energies in the cms $\sqrt{s_{NN}} = 4 \div 11 \text{ GeV}$, where it is expected the formation of nuclear matter at extreme densities and temperatures.[3]

Heavy Ion Linac (HILac)

Take a closer look to the heavy ion injector, for which transport channel will be built.

HILAC is intended to provide injection into the Booster heavy ions (eg, gold $^{197}\text{Au}^{31+}$) with an energy up to 3.2 MeV / n. It can accelerate beams of heavy ions with a charge to mass ratio $q / A \geq 1/6$ and peak currents up to 10 mA in a pulse duration of $8 \div 27$ microseconds at repetition rate up to 10 Hz.[1] As we can see in Figure 3.1 it consists of two IH – DTL and one RFQ sections with Krion-6T as an ion source.

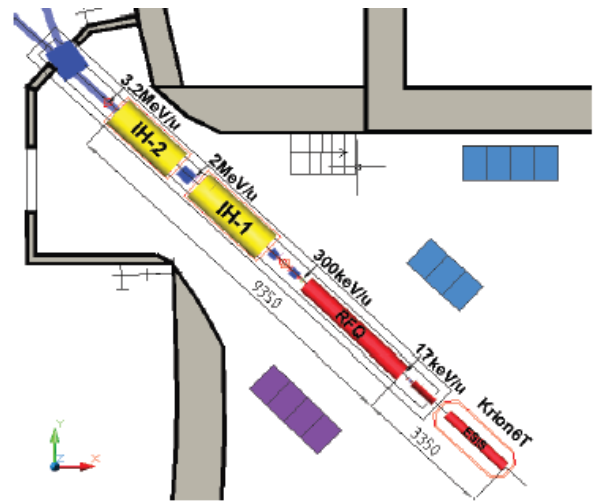


Figure 3.1 HILAC and its components

- Krion-6T



Figure 3.2 Krion-6T at high-voltage platform of LU-20 fore-injector. The Nuclotron Run #50.

Construction and assembly of Krion-6T were completed in 2013 and full-scale tests in reflex mode of operation had been started at a test bench. After reaching of 5.4 T of the solenoid magnetic field in a robust operation (the design value is 6 T) the $\text{Au}^{30+} \div \text{Au}^{32+}$ ion beams have been produced at intensity of about 6×10^8 particles per pulse. The required ionization time is 20 ms. Obtained parameters are close to required for HILAC operation. Thereafter the source was optimized for production of ions with charge to mass ratio of $q/A \geq 1/3$ in order to provide complex test of all its systems at operation on existing injection

facility. In May 2014 the source was installed at high Voltage (HV) platform of the LU-20 fore-injector (Figure 3.2) and used during Nuclotron run #50 in June. The main goal for future two years is to reach the project parameters of KRION-6T for Au^{31+} beam.[5]

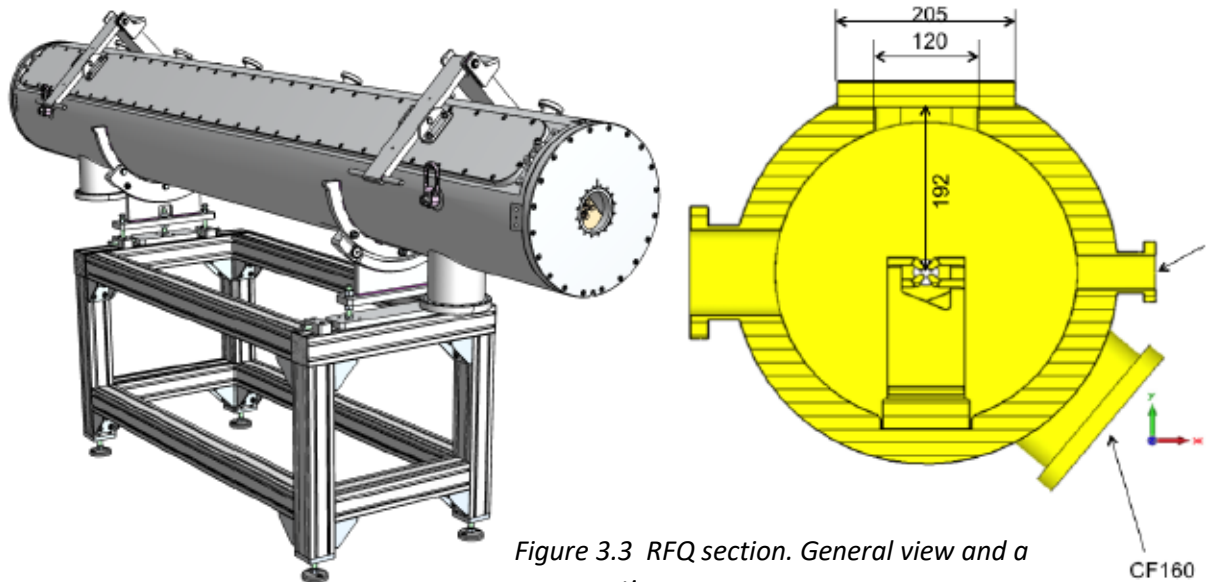


Figure 3.3 RFQ section. General view and a cross section.

Table 3.1: Fore-Injector RFO Parameters

- RFQ section

Parameter	Unit	Value
Input energy	keV/n	17
Output energy	keV/n	300
Operation frequency	MHz	100,625
Z/A	–	0,16
Current	mA	0 ÷ 10
Electrodes voltage	kV	70
Overall transmission	%	98
Aperture	Mm	5,2 ÷ 3,0

The beam formed by LEBT, enters $\beta\lambda/2$ accelerating structure with spatially uniform focusing quadrupole (RFQ). Due to the use RFQ is fact that such structure could provide a high overall transmission of the beam at low energy injection, his group and a further acceleration to the required parameters. RFQ electrodes are four-wire line (4-rod RFQ) in length with varying distance from the axis to the electrode surface and placed in a resonator working on the standing

wave type TEM_{110} . General view and a cross section of the section shown in Figure 3.3. Basic

parameters RFQ shown in Table 3.1. Resonator RFQ is a stainless steel cylinder with 3.1 m length and 50 mm wall thickness copper plating the internal surface of the electroplated. The resonator have 20 installed racks and four electrodes with applied modulation made of oxygen-free copper which are attached to them. Setting cells produced by moving the copper plate between the uprights.[1]

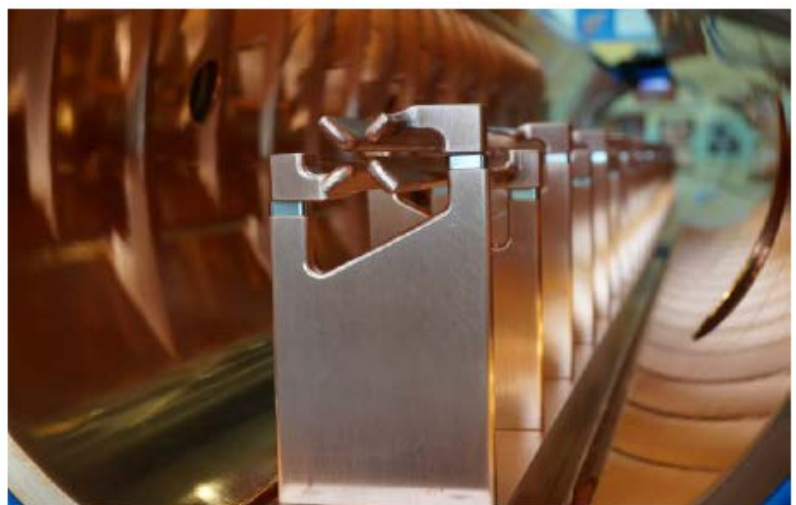


Figure 3.4 The 4 – Rod – RFQ

- IH – DTL sections.

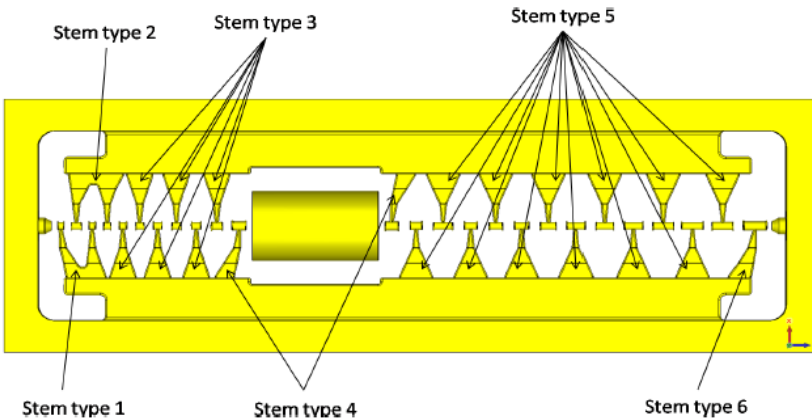


Figure 3.5 Drift tubes location in the structure IH1

Parameter	Unit	Value
Input energy	MeV/n	0,3
Output energy	MeV/n	2,0
Length	Cm	220
Operation frequency	MHz	100,625
$U_{eff}(A/Q = 6,5)$	MeV	10,46
$Q(real)$	–	20,000
$Z_{eff}(real)$	MOm/m	280
$P_c(real)$	kW	178
$P_{tot}(real), I = 10\text{ mA}$	kW	282
# Gaps	–	27
# Triplets	–	1

Table 3.2: Second accelerating section (IH1) parameters

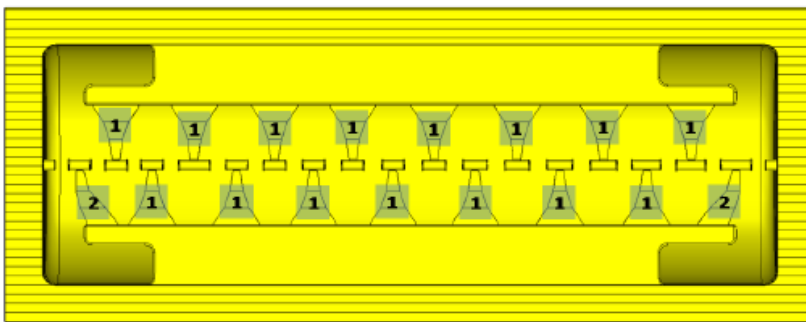


Figure 3.6 Drift tubes location in the structure IH2

Parameter	Unit	Value
Input energy	MeV/n	2,0
Output energy	MeV/n	3,2
Operation frequency	MHz	100,625
Length	Cm	191
$U_{eff}(A/Q = 6,5)$	MeV	8,00
$Q(real)$	–	25,000
$Z_{eff}(real)$	MOm/m	255
$P_c(real)$	kW	131
$P_{tot}(real), I = 10\text{mA}$	kW	211
# Gaps	–	18
# Triplets	–	0

Table 3.3: Third accelerating section (IH2) parameters

To further acceleration in the second and third sections there is a concept of accelerating structure KONUS (Kombinierte NULL grad Struktur - it.) - Combined with the structure of the zero-phase synchronous. It is $\beta\lambda / 2$ accelerating structure based on the drift tubes, working on the standing wave type TEM_{110} . The main feature of KONUS is separation each period net on sites with different tasks:

- main acceleration in the structure of a particle with zero synchronous asynchronous injection beam and the excess energy compared to the synchronous particle;
- transverse focusing quadrupole triplets or rotationally symmetric lenses;
- longitudinal focus grouped several gaps with synchronous phase up to 35° .

Thus, the total defocusing effect of high-frequency field is reduced, allowing the creation of a relatively long multigap section with "thin" drift tubes without focusing elements.[1]

Geometry of the transport channel

First step in transport channel design was to identify the key points on which the channel could be built. Significantly complicate the task – fact, that HILAC and Nuclotron located in different horizontal planes, so before finding the key points, it was decided to make the projection of LU-20 injection and the linear section NUCLOTON directions on the floor surface (Figure 4.1). After a selected direction were identified, the following values were determined:

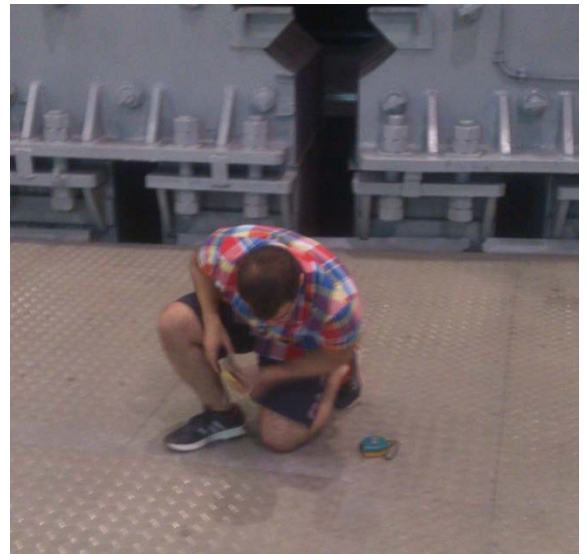


Figure 4.1 Applying key points on the floor surface

- Projection length of the Faraday cup (later, there will be rotary magnet instead of them, where beam will come from HILAC);
- Place for the first rotary magnet – beginning of the transportation channel;
- Angle between the HILAC and LU-20 line injection projections;
- Intersection between the perpendicular dropped on the HILAC axis and the continuation of the LU-20 injection axis;
- Height of objects relative to the floor's plane.



Figure 4.2 LU-20 injection + place for rotary magnet

The second step was the approximate construction of the channel geometry in AutoCAD 2012. It is important to note that at this stage, considered only the trajectory of the beam without longitudinal and transverse dynamics. Figure 4.3 shows the approximate location of a transport channel and position of rotary magnets on them.

Table 4.1 Transport channel parameters (Pre-version)

Parameter	Vertical rotation angle	Horizontal rotation angle	Rotation in space
First magnet	30°	-	30°
Second magnet	20,7°	6,3°	21,5°
Third magnet	12,6°	19,5°	22,0°
Straight section	768 cm		

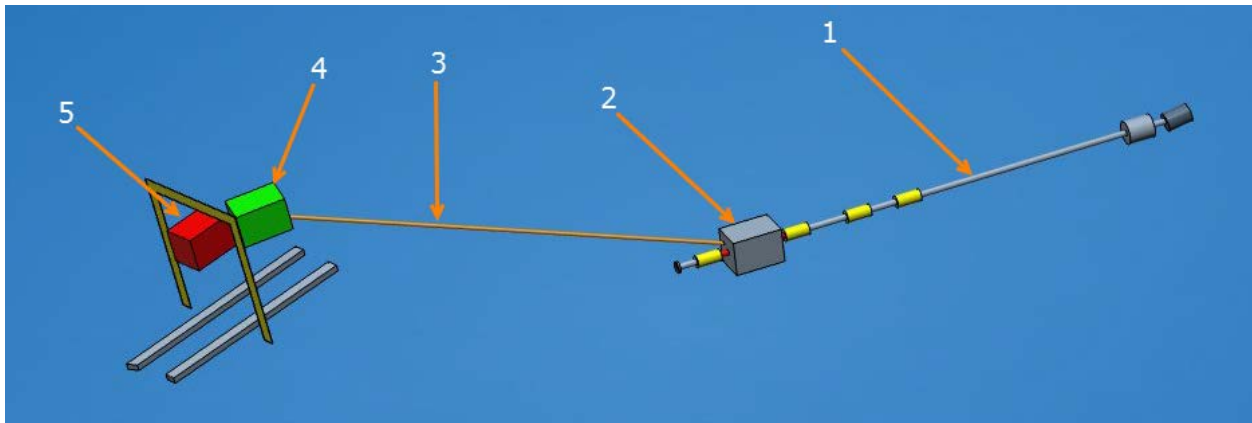


Figure 4.3 Transport channel HILAC-NUCLOTRON (Pre-version): 1 – LU-20 injection channel; 3 - Straight section of the transport channel; 2,4,5 – bending magnets.

Angle optimisation

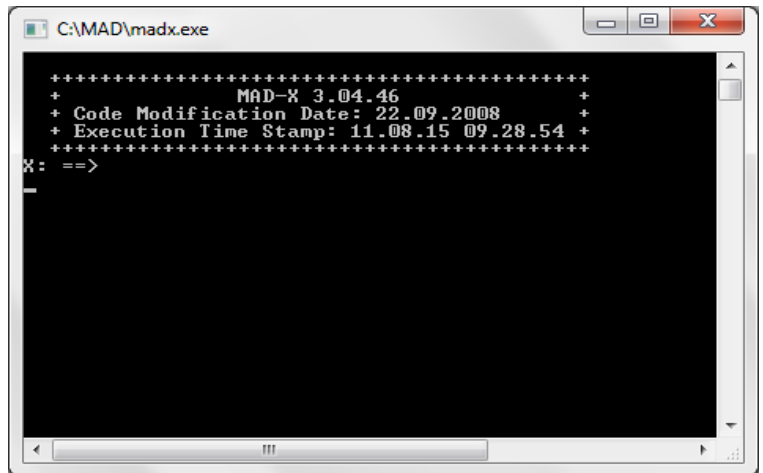
Before starting calculation of longitudinal and transverse dynamics, it is necessary to optimize the angles of rotation magnets in the channel. First of all, it is need to equalize the angls of those magnets, which in addition to the rotation of the beam have a through-span beam in a straight line: in first magnet - from HILAC to Booster, in the third - from the LU-20 to Nuclotron. Alignment angles also means minimizing the maximum of them. For the second magnet only condition is rotation angle top limit(we have it 30° degrees). It is based on magnet technical capabilities.

Table 5.1 Transport channel parameters (Optimisation)

First magnet	Rotation in space	15°	20°	21°	22°	23°	24°	25°	30°
Second magnet	Horizontal rotation angle	23,1°	17,5°	16,4°	15,3°	14,1°	13,0°	11,9°	6,3°
	Vertical rotation angle	21,9°	21,3°	21,2°	21,1°	21,1°	21,0°	20,9°	20,7°
	Rotation in space	30,4°	26,7°	26,0°	25,3°	24,7°	24,1°	23,6°	21,5°
Third magnet	Horizontal rotation angle	21,3°	20,7°	20,6°	20,5°	20,3°	20,2°	20,1°	19,5°
	Vertical rotation angle	12,6°	12,6°	12,6°	12,6°	12,6°	12,6°	12,6°	12,6°
	Rotation in space	23,4°	23,0°	22,9°	22,8°	22,7°	22,6°	22,5°	22,0°
Straight section, cm		778,202	774,512	773,808	773,114	772,431	771,758	771,095	767,914

Transport channel design in MAD-X

MAD is a project with a long history, aiming to be at the forefront of computational physics in the field of particle accelerator design and simulation. The MAD scripting language is *de facto* the standard to describe particle accelerators, simulate beam dynamics and optimize beam optics. MAD-X is the successor of MAD-8 and was first released in June, 2002. It offers most of the MAD-8 functionalities, with some additions, corrections, and extensions. The most important of these extensions is the Polymorphic Tracking Code (PTC) of E. Forest. MAD-X is released for the Linux, Mac OS X and Windows platforms for 32 bit and 64 bit architectures. The source code is written in C, C++, Fortran90 and Fortran77. The architecture of MAD-X is under complete review and reorganization in order to improve its maintainability, its flexibility and its performance. This long process should be completely transparent for the end users.[6]



Picture 6.1 MAD-X start

For using MAD-X program code (Figure 6.2) was written. The results presented in Figure 6.3.

```
title, "HILAC-Nuclotron channel v1";

!Section 1
dr1: drift, l = 1.146;
magn1: rbend, l = 0.816, angle = 0.4012;
dr2: drift, l = 0.1;
magn2: rbend, l = 0.816, angle = 0.4309, tilt = 0.99;
dr3: drift, l = 7;
magn3: rbend, l = 0.816, angle = 0.3960, tilt = -2.5748;
dr4: drift, l = 0.142;
sea: line=(dr1,magn1,dr2,magn2,dr3,magn3,dr4);

! Channel
bnch: line=(sea);

! Beam definition
/*Zion1 = 31;
Zion2 = 79;
Aion = 197;
Eion = 0.578;
beam, charge=Zion1*/
beam;

use, period=bnch;

survey, x0=0, y0=0, z0=0, theta0=0, phi0=0, psi0=0, file="Geom_res_v1.txt";

select, flag=save, full;
save, sequence=bnch, file="HN_Channel.seq";

stop;
```

Figure 6.2 Program code for MAD-X

```

@ NAME          %06s "SURVEY"
@ TYPE          %06s "SURVEY"
@ TITLE         %26s "HILAC-Nuclotron channel v1"
@ ORIGIN        %19s "MAD-X 3.04.46 Win32"
@ DATE          %08s "09/08/15"
@ TIME          %08s "12.45.03"
* NAME          S          L          ANGLE          X          Y          Z          THETA
$ %s            %1e          %1e          %1e          %1e          %1e          %1e          %1e
"BCH$START"    0          0          0          0          0          0          0
"DR1"          1.146        1.146        0          0          0          1.146        0
"MAGN1"        1.967498491    0.8214984911  0.4012    -0.1625939853  0          1.945636915    -0.4012
"DR2"          2.067498491    0.1          0          -0.2016463188  0          2.037696218    -0.4012
"MAGN2"        2.889845791    0.8223472995  0.4309    -0.6010641807  -0.1458449239  2.734151981    -0.6482845063  -0.
"DR3"          9.889845791    7            0          -4.561724499  -2.590235169  7.962739378    -0.6482845063  -0.
"MAGN3"        10.71120202    0.8213562315  0.396     -4.920372409  -2.79461357  8.666626547    -0.303732459  -0.
"DR4"          10.85320202    0.142        0          -4.962412315  -2.814769292  8.800754818    -0.303732459  -0.
"BCH$END"     10.85320202    0            0          -4.962412315  -2.814769292  8.800754818    -0.303732459  -0.

```

Figure 6.3 MAD-X results

After the coordinates being obtained in the global coordinate system, it was decided to check them in T-FLEX CAD.

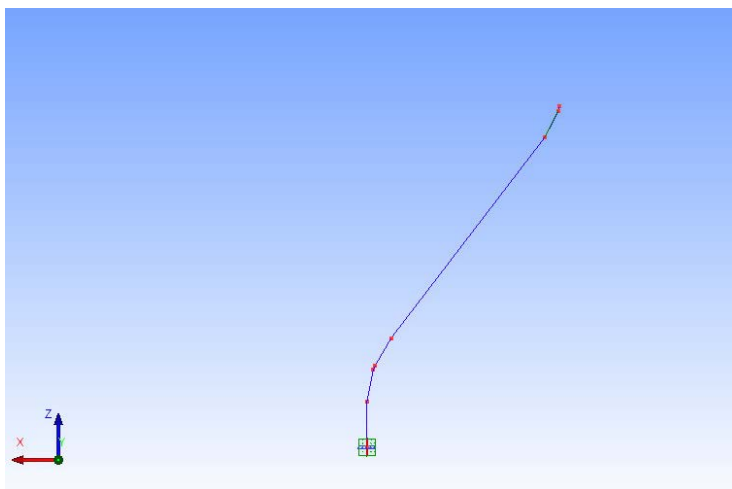


Figure 6.4 Top view

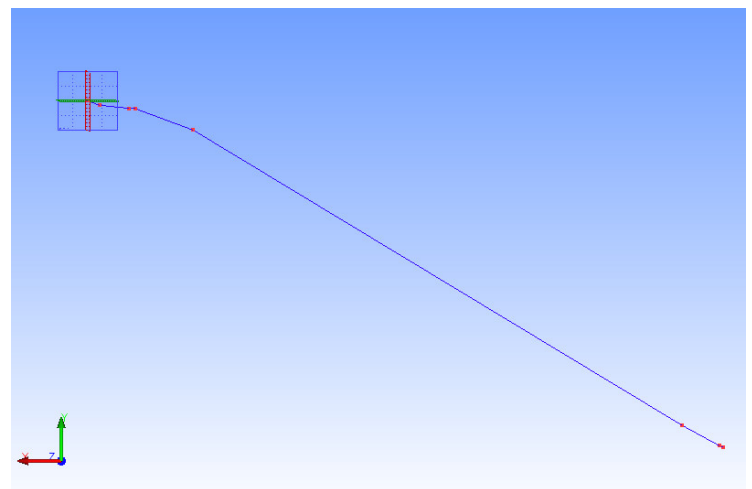


Figure 6.5 Back view

Table 6.1 Data verification from MAD-X model

		AutoCAD model	Result from MAD-X
First magnet	Rotation in space	23 ⁰	22,987 ⁰
Second magnet	Horizontal rotation angle	14,1 ⁰	14,157 ⁰
	Vertical rotation angle	21,1 ⁰	20,592 ⁰
	Rotation in space	24,7 ⁰	24,688 ⁰
Third magnet	Horizontal rotation angle	20,3 ⁰	19,741 ⁰
	Vertical rotation angle	12,621 ⁰	12,461 ⁰
	Rotation in space	22,7 ⁰	22,69 ⁰

Received data matches with a model from AutoCAD with high accuracy. Now, when the channel geometry constructed, should be considered longitudinal and transverse dynamics of the beam.

Beam dynamics

During the work was carried out the calculation of beam dynamics in the first approximation.

Random parameters were exhibited to lenses for each zones for estimate.

```
!Section 1
dr1: drift, l = 0.5;
q1: quadrupole, l = 0.29, k1=1;
dr2: drift, l = 0.3;
q2: quadrupole, l = 0.29, k1=-0.5;
dr3: drift, l = 0.5;
magn1: rbend, l = 0.647, angle = 0.4012;
dr4: drift, l = 0.1;
magn2: rbend, l = 0.647, angle = 0.4309, tilt = 0.99;
ra: srotation, angle = 0.04476332557;

!7 meter zone
dr5: drift, l=1;
q3: quadrupole, l = 0.29, k1=2;
dr6: drift, l=0.3;
q4: quadrupole, l = 0.29, k1=-0.1;
dr7: drift, l=2.29;
//q5: quadrupole, l = 0.29;
dr8: drift, l=0.59;
//q6: quadrupole, l = 0.29;
dr9: drift, l=0.3;
q7: quadrupole, l = 0.29, k1=0.2;
dr10: drift, l=0.7;
q8: quadrupole, l = 0.29, k1=-0.8;
dr11: drift, l=0.66;

!final section
magn3: rbend, l = 0.647, angle = 0.3960, tilt = -2.5748;
rb: srotation, angle = -0.04163037826;
dr12: drift, l = 0.142;
q9: quadrupole, l = 0.4;
dr13: drift, l = 0.65;
q10: quadrupole, l = 0.4;
dr14: drift, l = 0.45;
q11: quadrupole, l = 0.4;
dr15: drift, l = 3.5135;
magn4: sbend, l = 0.425, angle = 0.15874, tilt = -pi/2;
```

Also, the input parameters are optimized (match), to meet the given initial and final conditions (first and second line respectively).

```

match, SEQUENCE=bnch , betx=5.5 , alfx=-3.5, dx=0, dpx=0, bety=4, alfy=-3, dy=0, dpy=0;
constraint, range=#e, betx=3.245 , alfx=0.586, dx=1.746, dpx=0.259, bety=12.08, alfy=1.959, dy=0, dpy=0;
constraint, range=#s/#e, betx=30, bety=30;
//vary, name=q1->k1, step=1.0e-08, lower=-5.00 , upper=5.00 ;
//vary, name=q2->k1, step=1.0e-08, lower=-5.00 , upper=5.00 ;
vary, name=q3->k1, step=1.0e-08, lower=-5.00 , upper=5.00 ;
vary, name=q4->k1, step=1.0e-08, lower=-5.00 , upper=5.00 ;
//vary, name=q5->k1, step=1.0e-08, lower=-5.00 , upper=5.00 ;
//vary, name=q6->k1, step=1.0e-08, lower=-5.00 , upper=5.00 ;
vary, name=q7->k1, step=1.0e-08, lower=-5.00 , upper=5.00 ;
vary, name=q8->k1, step=1.0e-08, lower=-5.00 , upper=5.00 ;
vary, name=q9->k1, step=1.0e-08, lower=-5.00 , upper=5.00 ;
vary, name=q10->k1, step=1.0e-08, lower=-5.00 , upper=5.00 ;
vary, name=q11->k1, step=1.0e-08, lower=-5.00 , upper=5.00 ;
simplex, calls=1000000000, tolerance=0.000001;
endmatch;

```

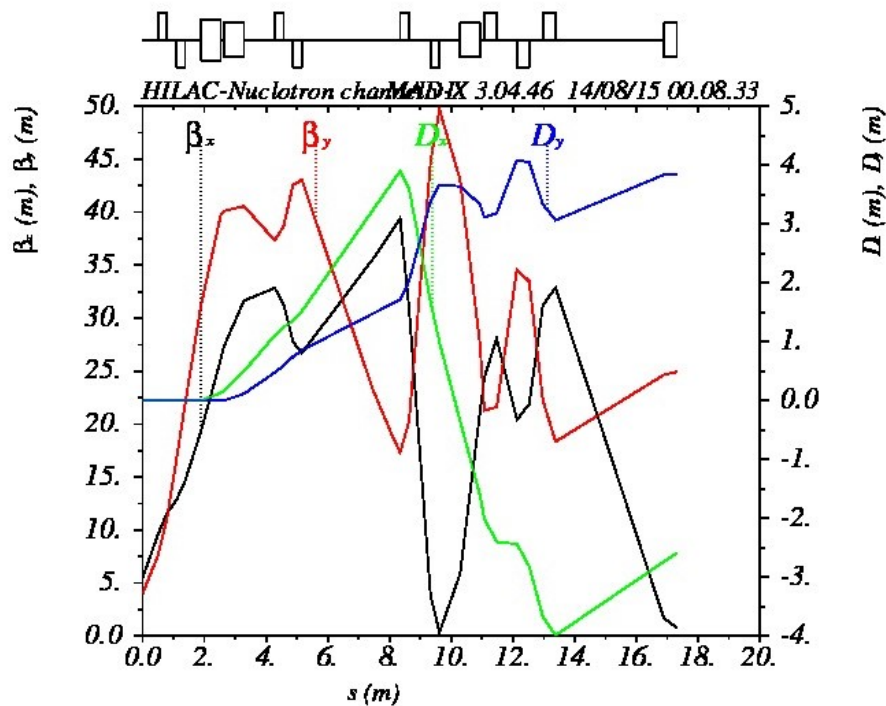
Optimized coefficients for a lens.

```

C:\Windows\system32\cmd.exe
2.79761463E+02
Final Penalty Function = 1.55921390e+004
Variable      Final Value  Initial Value  Lower Limit  Upper Limit
-----
q3->k1        7.05519e-001  2.00000e+000  -5.00000e+000  5.00000e+000
q4->k1       -9.30662e-001  -1.00000e-001  -5.00000e+000  5.00000e+000
q7->k1        3.14835e+000  2.00000e-001  -5.00000e+000  5.00000e+000
q8->k1       -1.91834e+000  -8.00000e-001  -5.00000e+000  5.00000e+000
q9->k1        1.99346e+000  0.00000e+000  -5.00000e+000  5.00000e+000
q10->k1       -1.78871e+000  0.00000e+000  -5.00000e+000  5.00000e+000
q11->k1       1.44124e+000  0.00000e+000  -5.00000e+000  5.00000e+000
END MATCH SUMMARY
VARIABLE "TAR" SET TO 1.55921390e+004

```

Graph dependencies beam parameters along the channel length.



Conclusions

- During the Summer Student Program at Joint Institute for Nuclear Research, introductory lectures and excursions were held;
- Complex of laboratory works for the course "Accelerator Technologies" was passed;
- Specialized course for NICA project was attended;
- Designed pre-version of transport channel between the linear accelerator HILAC and Nuclotron;
- Preliminary calculation of beam dynamics in the transport channel;

It should be noted, that the work on the transport channel design of is not completed. Subsequently, it will need more accurate harmonization of all parameters of the beam. Further work on the design of transport channel is planned to continue in the joint work of the RF Lab NRNU MEPhI and Veksler and Baldin Laboratory of High Energy Physics.

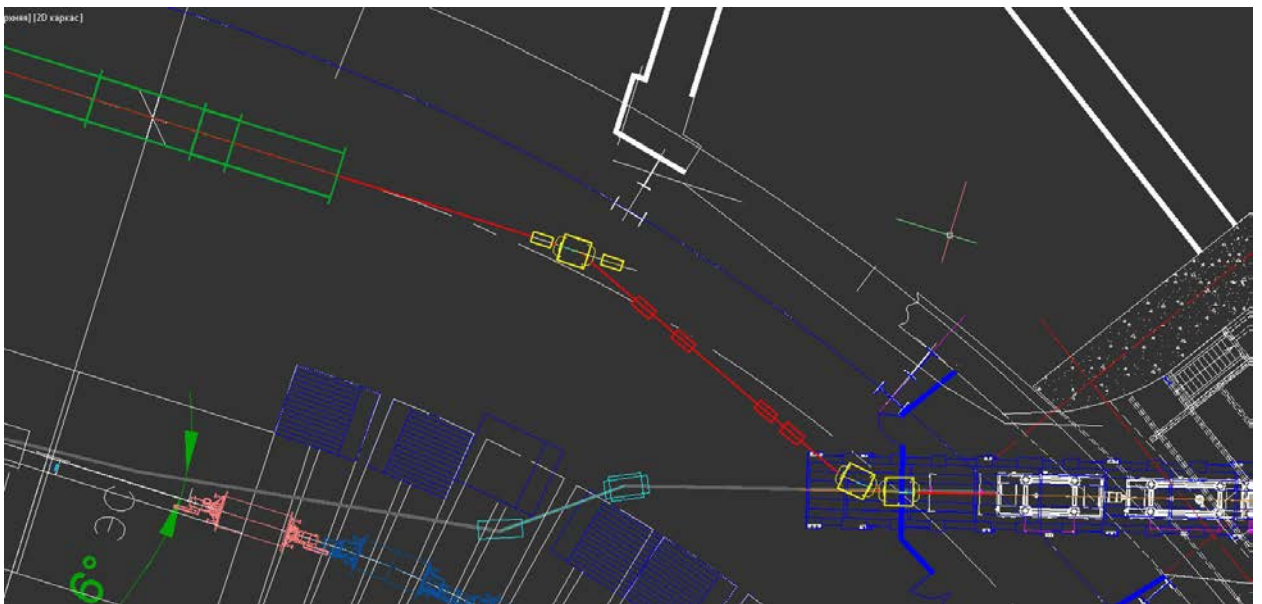


Figure 8.1 Transport channel HILAC – NUCLOTRON. Final version.

Acknowledgement

We would like to express our appreciation to PhD Butenko A.V and PhD Sidorin A.O, our practice supervisors and director of University Centre of Joint Institute for Nuclear Research, S. Z. Pakuliak, for giving us an opportunity to participate in Student Summer Program 2015.

We also wish to acknowledge the help provided by Tuzikov A.V for consulting us in our work.

In addition, we would like to express our gratitude to NIG UNC for the complex of laboratory works for the course "Accelerator Technologies", which we successfully completed. The knowledge acquired during this course significantly increased our engineering skills.

References

[1] NICA Technical Design Report, vol.1, Dubna 2015.

[2] NICA Technical Design Report, vol.2, Dubna 2015.

[3] NICA Technical Design Report, vol.3, Dubna 2015.

[4] NICA Technical Design Report, vol.4, Dubna 2015.

[5] A.V.Butenko et al., «The heavy ion linac at the NICA project», Proceedings of LINAC2014, Geneva, Switzerland

[6] <http://madx.web.cern.ch/madx/>

[7] A.V.Butenko et al., «Development of the NICA injection facility», Proceedings of IPAC2013, Shanghai, China